JOURNAL OF MATERIALS SCIENCE **36** (2001) 1951–1956

About the possible diminution of the sp^3 C presence along with the increase of the nitrogen enclosure in the CN_x thin films produced by reactive pulsed laser deposition

E. GYÖRGY, I. N. MIHAILESCU
Lasers Department, Institute of Atomic Physics, P.O. Box MG 54, 76900 Bucharest V, Romania

M. BALEVA, E. P. TRIFONOVA, M. ABRASHEV, V. DARAKCHIEVA
Sofia University, Faculty of Physics, 5 J. Boucher Blvd., 1164 Sofia, Bulgaria

A. ZOCCO, A. PERRONE
University of Lecce and Istituto Nazionale Fisica della Materia, Department of Physics, 73100 Lecce, Italy
E-mail: Alessio.Perrone@le.infn.it

We report herewith new experimental data concerning the synthesis of carbon-nitride thin films by reactive pulsed laser deposition ($\lambda = 248$ nm, $\tau_{FWHM} \leq 30$ ns) from a graphite target in low pressure nitrogen (0.2, 1 and 50 Pa) at a level of the incident laser fluence of 22 J/cm^2. The obtained structures were studied by Raman spectrometry and microhardness determinations. We have observed that an increase of the N_2 pressure leads to an increase in the N_2 content in the deposited films but causes the reduction of the amount of the sp^3 bounded C and the decrease of the microhardness of the obtained structures.

1. Introduction

Carbon nitride is a hypothetical material with unique potential properties. The original calculations by Liu and Cohen [1, 2] suggested that the bulk modulus of the theoretical covalent carbon-nitride solid, β-C_3N_4, with a structure similar to β-Si_3N_4, might significantly exceed that of diamond. Various deposition techniques such as reactive magnetron sputtering [3–6], chemical vapor deposition [7, 8], ion beam deposition [9] and ion plating [10, 11] have been applied in an attempt to grow carbon nitride thin films. Lasers have been also used for the synthesis and deposition of carbon-nitride thin films. The main approaches are reactive pulsed laser deposition (RPLD) [12–14] and laser chemical vapor deposition (LCVD) [15, 16]. The obvious advantage in this case is the ultimate purity of the deposited films as a consequence of their chemical synthesis with light. Numerical simulations were performed [17] in order to study the structure of the carbon-nitride solids.

We previously reported the synthesis and deposition of uniform and adherent, substoichiometric carbon-nitride (CN_x) thin films from a nuclear grade graphite target in low-pressure nitrogen or ammonia by RPLD using a XeCl* ($\lambda = 308$ nm, $\tau_{FWHM} \leq 30$ ns) excimer laser. We conducted the experiments with incident laser fluences 3, 6, 12 and 16 J/cm^2. The laser spot area was $S \cong 1$ mm^2. We observed the presence of the simple, double and, respectively, triple bonds between the C and N atoms. We found that the nitrogen enclosure inside the deposited films is clearly increasing as the incident laser fluence or the pressure of the chemically active gas (N_2 or NH_3) increased in the irradiation chamber [18–20]. In order to get a better insight into the influence of the enclosed nitrogen amount on the bond formation inside the growing films, we conducted new experiments at an increased level of the incident laser fluence of 22 J/cm^2. We report in this paper the results of the new analyses performed by Raman spectrometry and microhardness indentation of the films obtained at various ambient nitrogen pressures.

2. Experimental

The scheme of the experimental apparatus is outlined in Fig. 1.

Before each deposition the irradiation chamber was evacuated down to a residual pressure of $\sim 10^{-4}$ Pa and then filled with high purity nitrogen at three different dynamical pressures 0.2, 1 or 50 Pa. The pulses generated by a KrF* excimer laser source ($\lambda = 248$ mm, $\tau_{FWHM} = 25$ ns) running at 10 Hz were focused at 45° incidence angle. The targets used in the experiments were prepared from high purity (nuclear grade) graphite samples. The incident laser fluence was set at a value of $F_s \cong 22$ J/cm^2. Series of 10^4 laser pulses were applied to deposit one film. In order to avoid drilling the

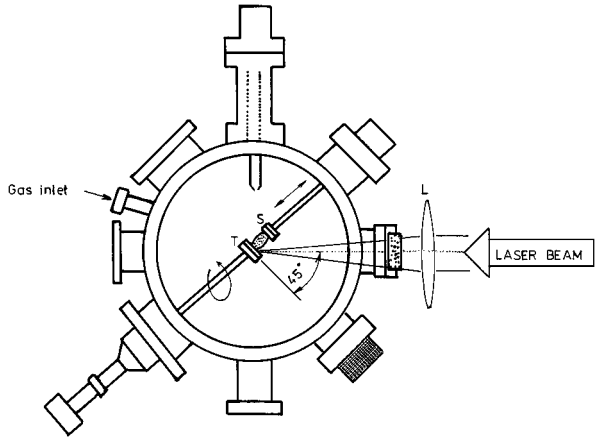

Figure 1 Experimental setup: L = lense, T = target and S = substrate.

target was rotated during the multipulse laser irradiation with the frequency of 3 Hz. The CN_x thin films having a thickness of a few hundreds of nm were deposited onto sapphire substrates. The collectors were not heated during the deposition. The target-collector separation distance was of 4 cm. After each deposition, the resulting structure was allowed to cool down in vacuum.

We recorded Raman spectra of the deposited films with a spectral resolution better than 5 cm^{-1}. We used SPEX 1403 double spectrometer equipped with a photomultiplier operating in a photon-counting mode. The setup was illuminated by a continuous wave Ar^+ laser source having a power of 60 mW and tunned on the 488 nm wavelength. The laser beam was focused in a spot having a diameter of about 200 μm.

Microhardness measurements were carried out with a PMT-3 microhardness tester equipped with diamond indentors both for Knoop and for Vickers determinations. The indentation pyramid was put in contact with the sample surface for 15 s. The investigations were conducted with loads P ranging from 1 to 200 g. The microhardness was calculated with the equation:

$$H\left[\frac{\text{kg}}{\text{mm}^2}\right] = B\frac{P[\text{kg}]}{d^2[\mu\text{m}^2]} \tag{1}$$

where $B = 14.229$ for the Knoop pyramid and $B = 1.854$ for the Vickers one, d is the measured imprint diagonal. The penetration depth (h) was calculated according to the equations:

$$h = d/30.51 \tag{2a}$$

$$h = d/7 \tag{2b}$$

for the Knoop and the Vickers indentor, respectively.

We mention that the use of the small loads as required for measuring the hardness of thin films, and thus small indentations can give rise to erroneous hardness values. This phenomenon is known as the indentation size effect (ISE). The development of a correct mechanism accounting for the ISE is a difficult task. This is due to the fact that the microhardness is strongly determined by the specific microstructures of the films and their surface status as well as by indentor geometry.

Recently [21] it was shown that a physically reasonable approach to deal with the ISE phenomenon is to assume an exponential dependence of the measured microhardness H on the indentation depth h of the type

$$H = H_\infty \pm A\exp\left(-\frac{h}{D_\text{p}}\right) \tag{3}$$

Here H_∞ is the load-independent hardness of the material and A is a constant related to the status of the sample surface. D_p is a quantity with meaning of deformation depth. As shown in Ref. [21] the ISE takes place whenever the indentor passes through a boundary between two different media, in particular through the film/substrate interface. We note, that the well-resolved singularities at the film/substrate border with respect to the microhardness-depth profiles of the films deposited at 1 Pa and 50 Pa N_2 pressures support these findings.

We can further write the contribution to the total microhardness value [22] of the film (with thickness D) and of the substrate, respectively, as:

$$H_\text{f} = H_{\text{f}\infty} \pm A^\text{fb}\exp\left(-\frac{h-D}{D_\text{p}^\text{fb}}\right) \tag{4}$$

$$H_\text{s} = H_{\text{s}\infty} \pm A^\text{s}\exp\left(-\frac{h-D}{D_\text{p}^\text{fb}}\right) \tag{5}$$

The quantities A^fb and D_p^fb characterize the film while A^s and D_p^s refer to the deposition substrate material.

When indentation hardness tests are conducted on a certain film/substrate structure the measurements reflect the contributions of the film and the substrate, since both of them are deformed under indentor load. All models describing the composite hardness involve appropriate distinction between the contribution of the film H_f and of the substrate H_s. In the most general approach proposed by Buckle [23] the composite hardness H_c of the film/substrate system is:

$$H_\text{c} = \alpha H_\text{f} + (1-\alpha)H_\text{s} \tag{6}$$

where the coefficient α depends on the film thickness.

According to [22] the coefficient α can be written as:

$$\alpha = \frac{1}{1+\exp\left(-\frac{h-D}{\Delta D}\right)} \tag{7}$$

where ΔD stands for an effective width of the transition region. For $h < D$, α is close to 1 and obviously $(1-\alpha) \to 0$. Correspondingly, the contribution of the film hardness to the composite one is prevalent. For $h > D, \alpha \to 0$ and $(1-\alpha) \to 1$. The contribution of the film hardness to the composite one decreases, so that deep down in the substrate the measured hardness becomes film and load-independent.

The recorded experimental dependence $H_\text{c}(h)$ of the uncoated sapphire substrate was modeled with Equation 3. The best fitting was obtained for the value $H_{\text{s}\infty}^\text{sapphire} = 13.1$ GPa. This value is in fairly good

agreement with the one obtained for Cr-dopped sapphire ($H_{s\infty}^{sapphire} = 10$ GPa) [24] and is of the order of that reported for single-crystalline sapphire samples ($H_{s\infty}^{sapphire} = 13.1$ GPa) [25].

3. Results

3.1. Raman studies

The Raman spectra within the wavenumber range from 300 to 2000 cm^{-1} of the three films deposited at different nitrogen pressures P_{N2} with subtracted baseline are shown in Fig. 2. The spectrum of the film obtained at the highest nitrogen pressure, 50 Pa (curve c in Fig. 2), like most spectra reported so far, exhibits two main peaks—the so called disorder (D) and graphite (G) bands, located at about 1360 and 1560 cm^{-1}, respectively. These features are usually assigned to the grahitic sp^2 bands—i.e. i. D band from in-plane vibrational modes at the domain surface and ii. the G-band arising from the E_{2g} mode of graphitic microdomains [26]. We note that, according to Ref. [27] when considering graphitic amorphous carbon as a continium random network (CRN) (where rings of clusters vibrations cannot be decoupled from the network in which they are embeded), inplane vibrational modes of $n = 4$—8 membered symmetric planar carbon rings with various frequencies ω can be determined. The interpretation of the Raman spectra of graphitic amorphous carbon [27] leads to the conclusion that the spectra comprise of about 20% $n = 5$ (E_2 modes with $\omega = 1100$ and 1529 cm^{-1}), 60% $n = 6$ (A_{1g} mode with $\omega = 1362$ cm^{-1} and E_{2g} mode with $\omega = 1581$ cm^{-1}) and about 20% $n = 7$(E_2 modes nearly degenerated with E_2 mode for $n = 5$). Thus G and D bands are formed mainly by A_{1g} ($\omega = 1362$ cm^{-1}) and E_{2g} ($\omega = 1581$ cm^{-1}) vibrational modes of $n = 6$ rings and their shapes are functions of $n = 5$ and $n = 7$ rings. The third, less intense, low frequency band which is visible in the spectrum of this film, peaking at about 700 cm^{-1}, is usually assigned to out-of-plane bending mode of graphite-like domains [28].

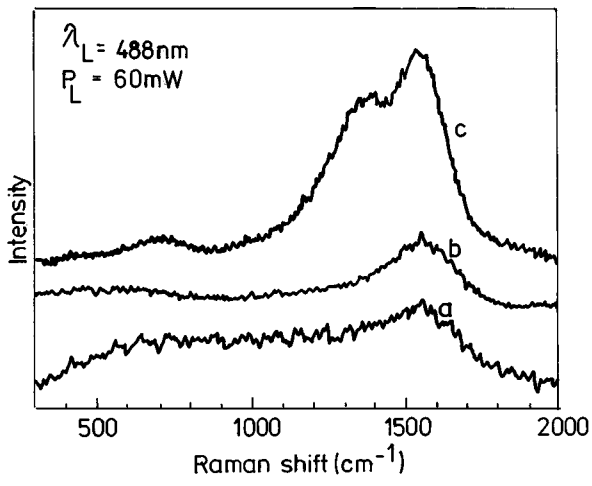

Figure 2 Raman spectra of the films deposited in low pressure nitrogen at 0.2 Pa (curve a), 1 Pa (curve b) and 50 Pa (curve c). We also give the decomposition of the spectrum into two mixed Lorentz-Gaussian profiles of the sample deposited at 50 Pa N_2 where the D- and G-bands could be well resolved.

In the spectra of the films, obtained at lower nitrogen pressures (curves a and b in Fig. 2), the D-band could not be clearly resolved. The very broad bands with a variable degree of disorder that are located around 1350 cm^{-1} and 1580 cm^{-1} are known to correspond to amorphous carbon [29]. Indeed, as has been pointed out in Ref. [29], the Raman spectrum of a-C is in fact a broadened variant of the graphite one. The maximum in the spectrum of a-C is peaking at about 1535 cm^{-1}, while the phonon frequency of the graphite is placed at 1575 cm^{-1}. Accordingly, the broad bands visible in the Raman spectra (curves a and b in Fig. 2) imply a high degree of amorphization. We mention that in the case of amorphous solids the Raman spectra are governed by the phonon density of states (PDOS).

The Raman spectra were decomposed in mixed Lorenz – Gaussian profiles (see e.g. curve c in Fig. 2 for the film deposited at 50 Pa N_2).

The results of the decomposition for all spectra are given in Table I. From Table I one observes that when increasing the gas pressure, the position of G-peak shifts toward higher frequencies (from 1560 to 1571 cm^{-1}) while its half-width narrows (from 155 to 80 cm^{-1}). The shift of G peak might be due to an increase of the amount of C = N stretching vibrations with frequencies in the range 1600–1700 cm^{-1} [30, 31] or to the increase of the strain in the graphitic rings, broken by incorporation of nitrogen atoms. According to the results recently reported by Bhattacharyya *et al.* [32], the ratio between the intensities of D and G peaks—I_D/I_G—increases with the nitrogen concentration, indicating an increase of the size of the sp^2 bonded carbon clusters. Taking into account that the increase of nitrogen pressure probably increases the fraction of $n = 5$ and $n = 7$ rings, one may conclude, that the increase of the nitrogen pressure leads to an increase of the amount of the sp^2 bonded carbon clusters. However, this does not cause the increase of their sizes.

On the other hand, Merkulov *et al.* [33] demonstrated that the Raman spectra of amorphous solids (such as diamond-like carbon (DLC)), obtained under a visible excitation are completely dominated by sp^2 C atoms. According to them, the Raman scattering in the ultraviolet (UV) region appears to be more suitable to providing a good estimation of PDOS when studying amorphous carbon.

Following the results from Ref. [32], we removed the high frequency peak, placed at about 1560 cm^{-1}. The substraction of the L_G profiles from the spectra allows the contribution of the sp^3 bonded atoms to become more apparent.

TABLE I The main parameters of the lines obtained by the decomposition of the Raman spectra corresponding to the films deposited at 0.2, 1 and 50 Pa N_2

P_{N2} [Pa]	Peak [cm^{-1}]	I_D/I_G	Half-width [cm^{-1}]
0.2	1560	0.18	155
	1367		68
1	1568	0.37	126
	1372		198
50	1571	0.83	80
	1377		162

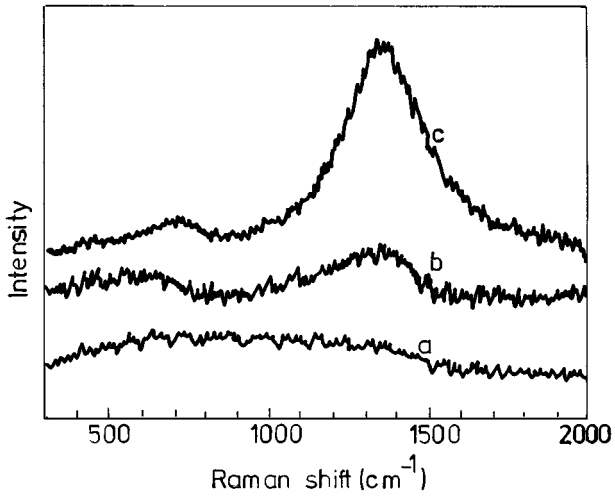

Figure 3 Subtracted Raman spectra of the samples deposited in low pressure nitrogen at 0.2 Pa (curve a), 1 Pa (curve b) and 50 Pa (curve c).

The subtracted spectra are shown in Fig. 3. The spectra of the films deposited at 1 Pa (curve b in Fig. 3) and 50 Pa (curve c in Fig. 3) N_2, similar with those reported by Merkulov *et al.* [33] for sputtered a-C, exhibit two characteristic features:

i. a broad peak at about 650 cm^{-1}, corresponding mostly to the bending motion of sp^2 C atoms with some possible contribution from sp^3 C sites and
ii. a band between 900 and 1550 cm^{-1}.

This second band could cumulate two contributions to the spectra: an sp^2 C network with the scattering at about 1400 cm^{-1} and sp^3 C network yielding a peak at about 1150 cm^{-1}. We notice, that the sp^3 contribution became visible after the afore described subtraction.

There is a strong resemblance between the spectrum of the film deposited at 50 Pa (curve c in Fig. 2) and the spectrum reported in Ref. [33] mainly containing 6 at.% sp^3 C. In both cases the band extending from 900 to 1550 cm^{-1} peaks at 1400 cm^{-1}.

Merkulov *et al.* [33] found that, with the increase of the sp^3 C at.% the maximum of the band shifts toward lower frequency values. Thus, this maximum is shifted to about 1300 cm^{-1} in the case of the film with 20 at.% sp^3 C and to 1150 cm^{-1} for the films with 30 and 75 at.% sp^3 C. Accordingly, the slight shift of this maximum (visible in Fig. 3) from 1400 cm^{-1}, for the film deposited at 50 Pa N_2 (curve c in Fig. 3) to 1350 cm^{-1}, for the film deposited at 1 Pa N_2 (curve b in Fig. 3), can be interpreted as an increase in the amount of the sp^3 C at.%.

In the spectrum obtained for the film deposited at 0.2 Pa N_2 (curve a in Fig. 3) the band between 900 and 1550 cm^{-1} could not be resolved. There is a strong shift of the maximum of this band toward lower frequencies. Thus, it can be concluded that the increase in ambient nitrogen pressure leads to a decrease of the sp^3 C at.%.

On the other hand, in our Raman spectra, obtained by using an Ar^+ laser source ($\lambda = 488$ nm) for excitation, the intensity of the bands strongly increases with the increase in nitrogen pressure. This fact can be attributed to the resonant enhancement of the scattering from the sp^2 C bonds in visible light [33, 34]. It is well known [33] that sp^2 network exibits resonance enhancement in the Raman cross-section because the local sp^2 C energy gap of about 2 eV is comparable with the energy of incident photons. The sp^3 C atoms do not exibit such a resonance effect because of the higher local gap of about 5.5 eV. Moreover, the strong increase in band intensity points to the increase of the sp^2 C at%.

3.2. Microhardness investigations

The experimental dependencies of the measured microhardness H_c(h) for the films deposited at 0.2 Pa (a), 1 Pa (b) and 50 Pa (c) N_2 and for the sapphire substrate (s), measured with the Knoop indentor, are shown in Fig. 4 by dots.

The microhardness-depth profile of the film deposited at 1 Pa N_2 (Fig. 5) was taken with the Vickers indentor as well.

The experimental recordings H_c(h), shown in Figs 4 and 5 were fitted with Equation 6 where H_f is given by Equation 4, H_s by Equation 5 and α by Equation 7. The numerically simulated dependencies are represented by full curves in Figs 4 and 5.

In order to infer the evolution of H_f(h) from the H_c(h) recording, we used the value of $H_{s\infty}^{\text{sapphire}} = 13.1$ GPa, determined from the modeling of the experimental H_c(h) recording of the uncoated substrate. The thickness D of the three layers have been measured with Tencor Alphastep 200 stylus profilometer. We obtained values of 600 nm, 510 nm and 320 nm for the films deposited at 0.2 Pa, 1 Pa and 50 Pa, respectively. The fitting parameters were $H_{f\infty}$, ΔD, A^{fb}, A^s, D_p^{fb}, D_p^s, A and D_p.

From Fig. 4, we observe, that the microhardness-depth profile of the film deposited at 1 Pa N_2 is entirely

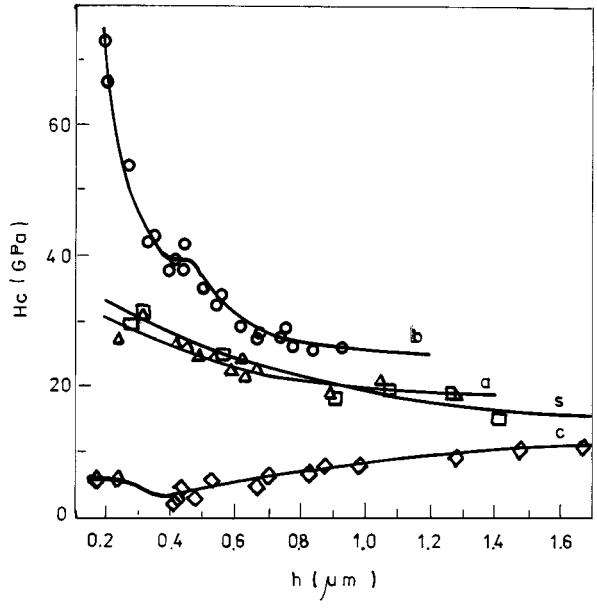

Figure 4 Microhardness values for the samples deposited in low pressure nitrogen at 0.2 Pa (a), 1 Pa (b), 50 Pa (c) and for the substrate (s) obtained with the Knoop indentor.

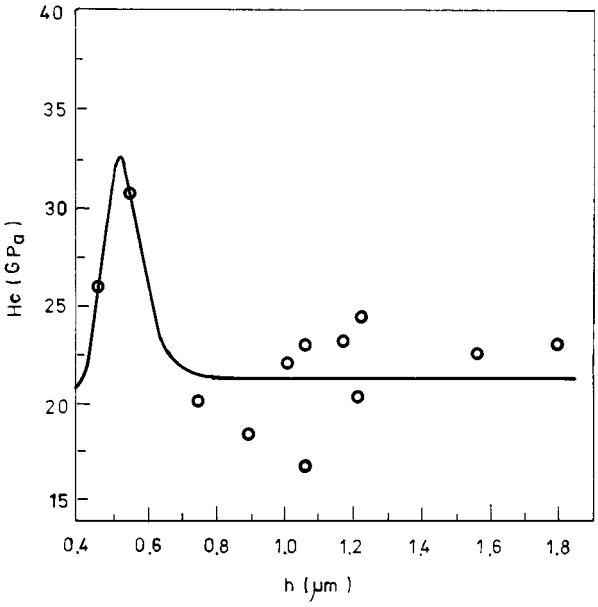

Figure 5 Microhardness values for the samples deposited at 1 Pa N_2 obtained with the Vickers indentor.

governed by the ISE on the surface (on the air/film boundary). This implies a very large value of the constant A, characterizing the status of the film surface or, in other words, a high hardness on the top of the film obtained at this pressure. Thus the actual value of the $H_{f\infty}$ cannot be reached even deep inside the film. The interpretation of the H_c(h) evolution of the film deposited at 1 Pa N_2, obtained with the Knoop indentor (curve b in Fig. 4) gave values of $H_{f\infty}$ ranging from 19.2 GPa to 35.6 GPa. In order to eliminate such a large uncertainty, we further used a Vickers indentor, having a smaller imprint area. The experimental recording H_c(h) of the film deposited at 1 Pa N_2, obtained with the Vickers indentor (see Fig. 5), significantly differs from the H_c(h) recording of the same sample, obtained with the Knoop indentor (Fig. 4). The best fitting of the experimental H_c(h) recording, given in Fig. 5, provided the value $H_{f\infty} = 19.4$ GPa.

On the other hand, the values of the load-independent hardness of the films deposited at 0.2 Pa and 50 Pa (curve a and c in Fig. 4), obtained from the fitting of the experimental recordings H_c(h) (Knoop indentor), provided values of $H_{f\infty} = 21.0$ GPa and of $H_{f\infty} = 5.6$ GPa, respectively. We therefore had no reason to repeat these determinations with the Vickers indentor. We note, that according to the current literature [35, 36] the microhardness value for diamond is within the range of 60–100 GPa and for graphite is much less than 1 GPa.

4. Discussions

We deposited carbo-nitride thin films at different ambient nitrogen pressures. In order to obtain low-compressibility (high-density) uniform and adherent hard films, with nitrogen content close to the predicted stoichiometric value, we increased the nitrogen pressure up to 50 Pa. Indeed, as reported elsewhere [37], we observed a strong increase in the N/C ratio from 0.20, for the film deposited at 1 Pa to 0.33, for the film obtained at 50 Pa.

On the other hand, our new results are in good agreement with the molecular-dynamics simulation reported by F. Weich *et al.* [17]. The authors of this paper performed numerical calculations in order to systematically study the amorphous state of carbon-nitrides for a wide range of stoichiometries and densities. They considered periodically repeated supercells with 140 atoms. A total of 60 amorphous supercells with 6 different densities, 1.5, 2.0, 2.5, 3.0, 3.5 and 4.0 g/cm^3 was taken into account. The N concentration was varied from 0% to 57% (the last value corresponding to the nitrogen amount in the ideal β-C_3N_4 compound). In apparent contradiction with the calculations of Liu and Cohen, their main results can be summarized as follows.

i. The densities of the films decrease with increasing N-incorporation concentrations, a trend which will inhibit the synthesis of any novel high-density, low-compressibility and very hard CN material.

ii. The N-C coordination number decreases with the increase of the N content. As a consequence, the enclosure of a large amount of N would result in a structure exhibiting stronger π peaks, indicating an increasing number of double and triple bonds, instead the single bonds, characteristic for the β-C_3N_4 molecule.

iii. The addition of N drastically lowers the C-sp^3 content. This third prediction limits the potential formation of β-C_3N_4 molecule. We note that in order to obtain a low-compressibility very hard β-C_3N_4 phase, the carbons should be totally sp^3—while all nitrogen should be sp^2 bonded.

Our Raman studies show that the increase in nitrogen pressure in the irradiation chamber which causes the increase of the N content of the films [37] results in a decrease of the sp^3 C at%. The sp^2 hybridization of the C atoms becomes dominant in the films deposited at higher nitrogen pressures (50 Pa) which are richer in N.

In accordance with these predictions [17] and evolutions, the hardness values of the films deposited at low nitrogen pressure ($P_{N2} = 0.2$ Pa and 1 Pa, respectively) are close to each other and much higher than that for the film grown at $P_{N2} = 50$ Pa. Indeed, the pressure increase to 50 Pa leads to a sharp (about threefold) decrease of the film hardness. This finding is in agreement with the results of Raman scattering, indicating a high degree of graphitization along with the increase in nitrogen pressure during deposition. We also observed that the microhardness decrease can be the effect of the density decrease in the films deposited at higher pressures, which grow more fluffy.

5. Conclusions

We deposited CN_x thin films by RPLD from a graphite target in nitrogen at 0.2, 1 and 50 Pa. In comparison with previous depositions we increased the incident laser fluence at 22 J/cm^2. The increase in nitrogen pressure

causes a higher nitrogen incorporation in the films. On the other hand, the increase in nitrogen content leads to the reduction of the sp^3-bonded C. This reduction is most probably responsible for the strong microhardness decrease when the nitrogen pressure is increased from 0.2 Pa to 50 Pa.

We consider, that these results basically support the prediction made in [17], namely that the addition of nitrogen lowers the sp^3 hybridized C content. This strongly overcomes in our opinion the successful synthesis of low-compressibility, high density, very hard β-C_3N_4 structure.

Acknowledgements

The microhardness measurements are supported by The Bulgarian National Fund for Scientific Investigations under contracts Φ-521 (1995). The authors are grateful to Professor Armando Luches from the Department of Physics, University of Lecce for encouraging and useful scientific discussions. Ion N. Mihailescu thanks to Consiglio Nazionale della Ricerca (CNR) for the financial support through a CNR-NATO fellowship which made possible his participation in this work. Enikö György acknowledges with thanks the financial support of CNR in the framework of the bilateral agreement with the Romanian Ministry of Research and Technology and to the Istituto Nazionale per la Fisica della Materia for a research contract which ensured her participation to the work.

References

1. A. Y. LIU and M. L. COHEN, *Science* **245** (1989) 841.
2. *Idem., Phys. Rev. B* **41** (1990) 10727.
3. K. M. YU, M. L. COHEN, E. E. HALLER, W. L. HANSEN, A. Y. LIU and I. C. WU, *Phys. Rev. B* **49** (1994) 5034.
4. H. SJOSTROM, I. IVANOV, M. JOHANSSON, L. HULTMAN, J. E. SUNDGREN, S. V. HAINSWORTH, T. F. PAGE and L. R. WALLENBERG, *Thin Solid Films* **246** (1994) 103.
5. H. SJOSTROM, L. HULTMAN, J. E. SUNDGREN, S. V. HAINSWORTH, T. F. PAGE and G. S. A. M. THEUNISSEN, *J. Vac. Sci. Technol. A* **14**(1) (1996) 56.
6. A. CZYZNIEWSKI, W. PRECHT, M. PANCIELEJKO, P. MYSLINSKI and W. WALKOWIAK, *Thin Solid Films* **317** (1998) 384.
7. Y. ZHANG, Z. ZHOU and H. LI, *Appl. Phys. Lett.* **68**(5) (1996) 634.
8. L. C. CHEN, D. M. BHUSARI, C. Y. YANG, K. H. CHEN, T. J. CHUANG, M. C. LIN, C. K. CHEN and Y. F. HUANG, *Thin Solid Films* **303** (1997) 66.
9. K. OGATA, J. F. D. CHUBACI and F. FUJIMOTO, *J. Appl. Phys.* **76** (1994) 3791.
10. Y. TAKI, T. KITAGAWA and O. TAKAI, *Proc. Symp. Plasma Sci. Mater.* **8** (1995) 39.
11. O. TAKAI, Y. TAKI and T. KITAGAWA, *Thin Solid Films* **317** (1998) 380.
12. C. NIU, Y. Z. LU and C. M. LIEBER, *Science* **261** (1993) 334.
13. J. BULIR, M. JELINEK, V. VORLICEK, J. ZEMEK and V. PERINA, *Thin Solid Films* **292** (1997) 318.
14. C. W. ONG, X. A. ZHAO, Y. C. TSANG, C. L. CHOY and P. W. CHAN, *J. Mater. Sci.* **32** (1997) 2347.
15. R. ALEXANDRESCU, R. CIREASA, G. PUGNA, A. CRUNTEANU, S. PETCU, I. MORJAN, I. N. MIHAILESCU and A. ANDREI, *Appl. Surf. Sci.* **109** (1997) 544.
16. A. R. CIREASA, R. A. CRUNTEANU, I. MORJAN, C. MARTIN and I. N. MIHAILESCU, in E-MRS Spring Meeting Symposium A (June 1997).
17. F. WEICH, J. WIDANY and TH. FRAUENHEIM, *Phys. Rev. Lett.* **78**(17) (1997) 3326.
18. I. N. MIHAILESCU, E. GYORGY, R. ALEXANDRESCU, A. LUCHES, A. PERRONE, C. GHICA, J. WERCKMANN, I. COJOCARU and V. CHUMAS, *Thin Solid Films* **323**(1, 2) (1998) 72.
19. A. P. CARICATO, G. LEGGIERI, A. LUCHES, A. PERRONE, E. GYORGY, I. N. MIHAILESCU, M. POPESCU, G. BARUCCA, P. MENGUCCI, J. ZEMEK and M. TRCHOVA, *ibid.* **307** (1997) 54.
20. M. L. DE GIORGI, G. LEGGIERI, A. LUCHES, M. MARTINO, A. PERRONE, A. ZOCCO, G. BARUCCA, G. MAJNI, E. GYORGY, I. N. MIHAILESCU and M. POPESCU, *Applied Surface Science* **127** (1998) 481.
21. M. BALEVA, E. MATEEVA and E. P. TRIFONOVA, *J. Mater. Sci.* **33** (1998) 1.
22. M. BALEVA, V. DARAKTCHIEVA, E. GORANOVA and E. P. TRIFONOVA, in Proceedings of 18th Greek-Bulgarian Symposium on Semiconductor, February, 1999 (Thessaloniki, Greece); *J. Mater. Sci.*, submitted.
23. H. BUCKLE, "The Science of Hardness Testing and its Research Applications" (American Society for Metals, Metals Park, OH, 1973) p. 453.
24. H. J. WEISS, A. KRELL and B. MULER, *Phy. Stat. Sol. (a)* **93** (1986) 509.
25. W. C. OLIVER and G. M. PHARR, *J. Mater. Res.* **7** (1992) 1564.
26. N. NAKAYAMA, Y. TSUSHIYA, S. TAMADA, K. KOSUGE, K. TAKAHIRO and S. YAMAGUCHI, *Jpn. J. Appl. Phys. Lett.* **32** (1993) L1465.
27. T. E. DOYLE and J. R. DENNISON, *Phys. Rev. B* **51**(1) (1995) 196.
28. PHAM V. HUONG, *Diamond and Related Materials* **1** (1991) 33.
29. J. E. SMITH, M. H. BRODSKY, B. L. CROWDER and M. I. NATHAN, *J. Non-Cryst. Solids* **8–10** (1972) 179.
30. M. P. SIEGAL, L. J. MARTINEZ-MIRANDA, N. J. DINARDO, D. R. TALLANT, J. C. BARBOUR and P. NEWCOMER PROVENCIO, in the SPIE Proceedings of the Symposium High Power Laser Ablation (Santa Fe, New Mexico, April 26–30, 1998) to be published.
31. D. LIN-VIEN, N. B. COLTHUP, W. G. FATELEY and J. G. GRASSELLI, "The Handbook of Infrared and Raman Characteristic Frequencies of Organic Molecules" (Academic Press, Inc., 1991).
32. S. BHATTACHAYYA, J. HONG and G. TURBAN, *J. Appl. Phys.* **83**(7) (1998) 3917.
33. V. I. MERKULOV, J. S. LANNING, C. H. MUNRO, S. A. ASHER, V. S. VEERASAMY and W. I. MILNE, *Phys. Rev. Lett.* **78**(25) (1997) 4869.
34. K. W. GILKES, H. S. SANDS, D. N. BATCHELDER, J. ROBERTSON and W. I. MILNE, *Appl. Phys. Lett.* **70**(15) (1997) 1980.
35. J. J. GILMAN, in "Science of Testing and its Research Applications," edited by J. H. Wesrbrook and H. Conrad (American Society for Metals, Metals Park, OH, 1973) p. 51.
36. P. K. ACHMANN, D. LEERS and H. LYDTIN, *Diamond and Related Materials* **1** (1991) 1.
37. A. ZOCCO, A. PERRONE, E. D'ANNA, G. LEGGIERI, A. LUCHES, R. KLINI, I. ZERGIOTI and C. FOTAKIS, *ibid.* **8** (1999) 582.

Received 8 March
and accepted 15 September 2000